Agglomeration of self-interstitials in Si observed at 450 °C by high-resolution transmission electron microscopy

S. Takeda
Department of Physics, Faculty of Science, Osaka University, 1-16 Machikane-yama, Toyonaka, Osaka 560, Japan

T. Kamino
Techno Research Laboratory, Hitachi Instruments Engineering Company, Ltd., 882 Ichige, Katsuta-shi, Ibaraki 312, Japan
(Received 19 September 1994)

We have observed an early stage of agglomeration of self-interstitial atoms in a Czochralski-Si crystal by high-resolution transmission electron microscopy at 450 °C. Based on analyses of the experimental data, it has been suggested that self-interstititals, introduced by electron (300 keV) irradiation, are first arranged along the ⟨110⟩ direction, forming a linear interstitial defect structure that has no dangling bond in the {110} cross section. After the nucleation, the defect is extended on the {113}-type plane.

I. INTRODUCTION

The extremely mobile self-interstitials[1] in a Si crystal are point defects usually detected only as an agglomerate. The agglomeration is commonly introduced in the temperature range up to about 1200 °C by various processes, in particular during the fabrication of electronic devices, thereby arousing much interest. Even though extensive studies have thus far shown the spatial distribution, morphology, structures, and growth conditions of the various kinds of the agglomerates, the early stage of agglomeration has not yet been revealed at the atomic level. A number of studies[2,3] have indicated that the agglomeration of self-interstitials at lower temperature (350–650 °C) is related to the existence of foreign atoms such as oxygen and carbon. Furthermore, recent studies[4,5] on thermal donors, which are formed by annealing at about 450 °C and have been most extensively investigated in the past decade, have suggested that a self-interstitial is involved as well as oxygen atoms. The results thus lead further studies toward the understanding and controlling of the agglomeration at the atomic level.

Self-interstitials in our experiment were introduced by atomic displacement due to elastic electron scattering, which is an established means to create points defects in a Si crystal.[1] The threshold electron energy needed to create the Frenkel pairs in Si is estimated at about 170 keV. Therefore, the incident electrons (300 keV) in the transmission electron microscope that we used had two roles; some transfer their energy to create the Frenkel pairs, and others undergo small-angle scattering and form high-resolution transmission electron microscopy (HRTEM) images through the conventional electron optics. The aim of this pair is to present the atomic structure of a small cluster of self-interstitials observed by HRTEM at 450 °C. It is worth noting that near this temperature the agglomeration of self-interstitials is enhanced,[2,3,6,7] as well as the formation of the thermal donors.[4,5,8]

II. EXPERIMENTAL DETAILS

The Si specimen that we examined was Czochralski (Cz) silicon wafers, *p* type, 1–20 Ω cm. The fragments of the Si crystal were supported on a wire filament of the hot specimen holder.[9] The electron irradiation and observation was carried out at 450 °C by a high-resolution electron microscope (300 kV) with ⟨110⟩ incidence. During the observation, the specimen surfaces were not controlled. The flux of electrons was estimated to be 5×10^{24} electrons $s^{-1}m^{-2}$ on the specimen surface and the displacement cross section of a Si atom was roughly estimated to be 20×10^{-28} m^2.

In order to analyze the atomic structure of a small defect embedded inside a thin foil in a convincing way, we also present a HRTEM image of a defect of the same kind observed in a specimen which was prepared by an alternative technique. The specimen was first irradiated by electrons (2 MeV) at 450 °C, the estimated flux being 1×10^{24} electrons $m^{-2}s^{-1}$. The specimen was then polished by Ar-ion etching after electron irradiation; the observed defect is no longer embedded inside the thin foil but penetrates it. The specimen was examined stably by HRTEM with 160 keV electrons at room temperature.

III. RESULTS

A sequence of the *in situ* HRTEM observation at 450 °C is depicted in Fig. 1. After irradiation for 600 s [Fig. 1(a)], no detectable change took place in the specimen. After prolonged irradiation for 1080 s [Fig. 1(b)], we find that a few defects grew in the same irradiated area. They are marked by 1 and 2. Defect 1 in a thinner part was just at an early stage of growth, and defect 2 in a thicker part was already extended on a {113}-type plane. No bend was yet observed in the planar defect, which fact implies that the defect at the early stage possesses no twofold axis with regards to ⟨001⟩. After irradiation for 1260 s [Fig. 1(c)], the defects further developed, and

another defect of the same kind marked by 3 appeared. The defect on {113} has commonly been introduced by annealing, electron irradiation, and ion implantation, and was already identified to be an agglomerate of self-interstitials.[7,10,11] It is well known that the defect has a strong tendency to grow preferentially along the ⟨110⟩ direction.[7,10]

We closely examine the early stage of the agglomeration. Figure 2 shows the enlarged images of the same area taken from Fig. 1, revealing the growth process of defect 1. The images after irradiation for 1080 [Fig. 2(b)] and 1260 s [Fig. 2(c)] clearly show the disturbance in the regular lattice, whereas no disturbance is detected after irradiation for 600 s [Fig. 2(a)]. In order to extract an unknown atomic configuration of the defect which is embedded inside a crystal, an image processing technique was applied as described in the Appendix. Hence the image contrast due to the defects is only observable in the corresponding processed images [Figs. 2(d), 2(e), and 2(f)]. It is evident that the characteristic twofold image patterns (indicated by the longer arrows) appear after electron irradiation for 1080 [Fig. 2(e)] and 1260 s [Fig. 2(f)]. Each pattern consists of the dark region at the middle and the four bright spots, two of which are at the left and the right, and the other of which at the top and the bottom are dimmer. In order to clarify the atomic structure resulting in the characteristic pattern in a convincing way, we next present the HRTEM image of a defect of the same kind observed at room temperature, before analyzing the *in situ* images further.

Figure 3(a) depicts the [110] cross section of a defect, which was found, along with more extended defects on {113}, in an electron (2 MeV)-irradiated area of the same kind of specimen as in the *in situ* observation. The irradiation was performed at 450 °C. After introducing defects, we examined the specimen stably by HRTEM with 160-keV electrons at room temperature. The observed defect is no longer embedded inside the thin foil (whose thickness is about 7 nm), but penetrates it. Figure 3(a) was processed by the Fourier filtering, and the result is shown in Fig. 3(c). The three characteristic twofold patterns, similar to those found in the *in situ* images, line up along the horizontal direction, being bounded by a perfect crys-

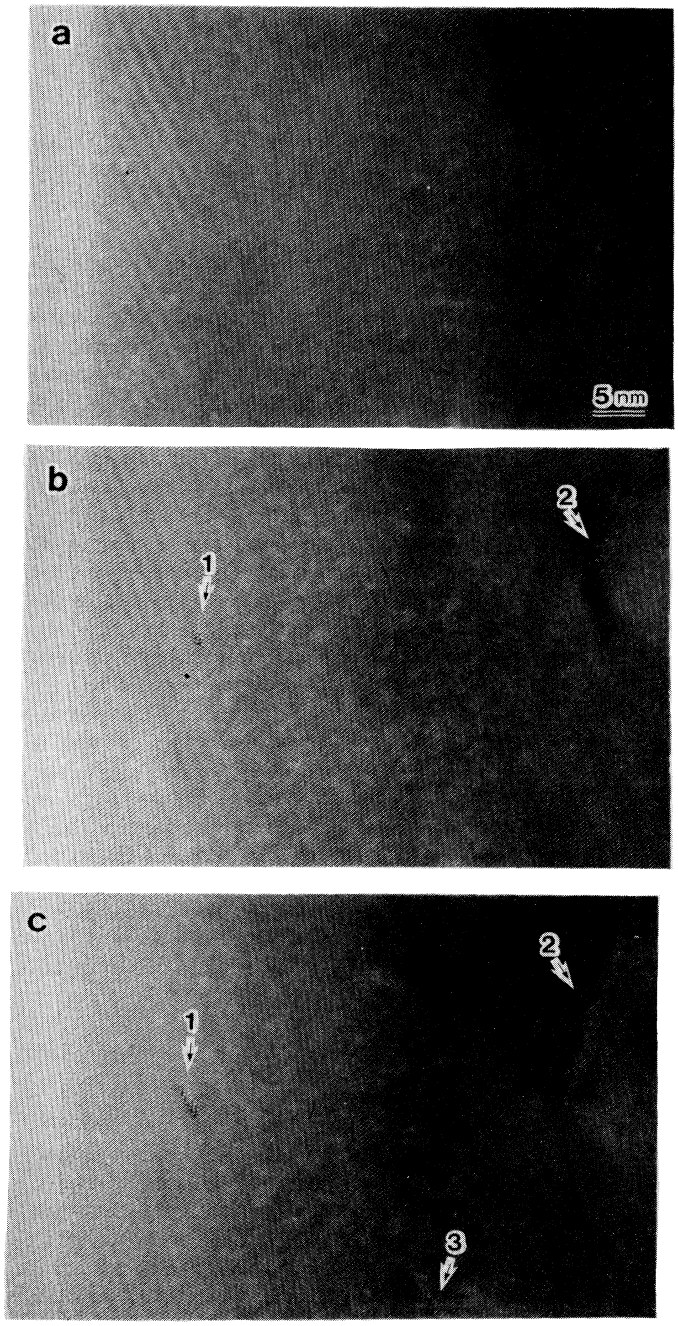

FIG. 1. Agglomeration process revealed by *in situ* HRTEM (300 kV) observation at 450 °C.

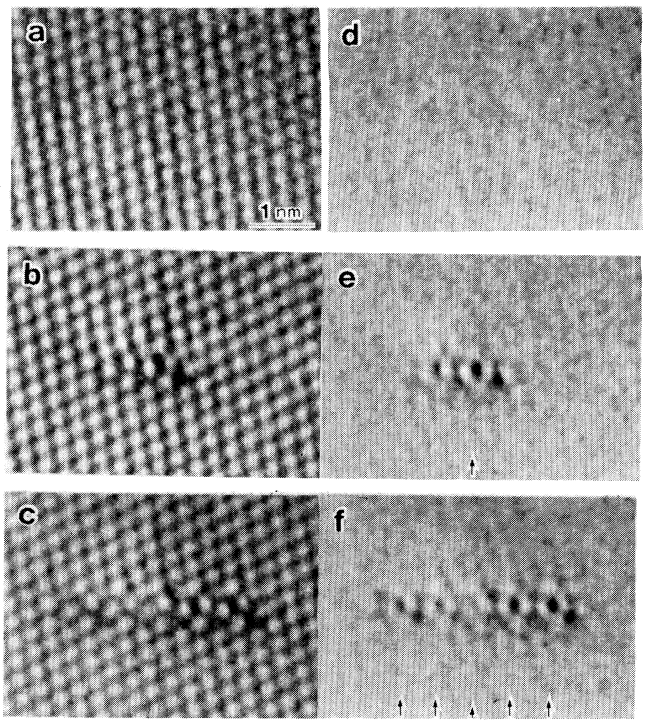

FIG. 2. Enlarged and processed images of the agglomerate 1 seen in Fig. 1.

tal. We have found that this linear defect structure along [110] can be represented as ...*PEIIIEP*... by notation[12] which was defined in a previous theoretical study to describe the extended {113} defect structure. Here *I*, *E* and *P*, respectively, denote the structural unit incorporated with a chain of the additional atoms (agglomerated self-interstitials), that of the edge along [110], and that of the perfect crystal. The model is confirmed by the accurate image simulation [Fig. 3(b)]. The assumed parameters in Fig. 3(b) are as follows: the specimen thickness is 7 nm, Cs is 0.8 mm, the amount of defocus is 55 nm (Scherzer defocus), the standard deviation of defocus is 5 nm, the beam convergence is 0.5 nm^{-1}, and the objective aperture radius is $1/0.15$ nm^{-1}. The observation at room temperature has shown that (1) the twofold pattern arises from the *I* unit, and (2) the linear defect configuration is stable even though the observed structure, seen in the (110) cross section, is probably a part of extremely extended defects. The observation at room temperature concerning the extremely extended defects has been reported elsewhere.[13]

With a key to analyze the images, we now return to the *in situ* observation (Fig. 2). The twofold pattern that appeared after irradiation for 1080 s [Fig. 2(b) and 2(e)] indicates that a linear defect structure, represented by ...*PEIEP*... was already formed inside the thin foil. We call a family of possible defect structures represented by ...*PEIEP*..., ..*PEIIEP*..., and ...*PEIIIEP*..., respectively, single line interstitial defect (LID), doubled LID, and tripled LID structures, in which a few additional atom chains along the ⟨110⟩ direction are inserted in a regular lattice. The single LID structure, whose atomic coordination was originally given[14] in a speculative

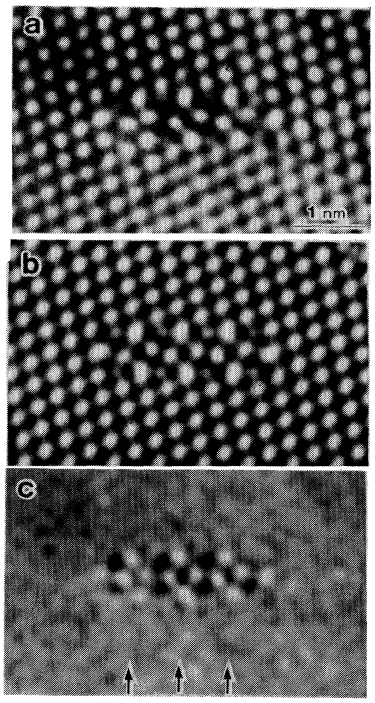

FIG. 3. Defect due to electron (2 MeV) irradiation at 450 °C observed with 160 keV electrons at room temperature.

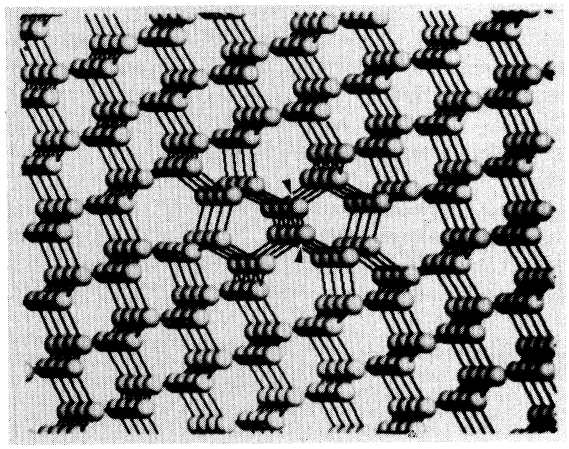

FIG. 4. The line interstitial defect configuration incorporated with self-interstitials in Si. The chain of additional Si atoms is marked by the arrow heads.

manner, is reproduced in Fig. 4. It possesses the periodicity of $\langle 110 \rangle a/2$ along ⟨110⟩, *a* being the lattice parameter of a Si crystal. The image pattern in Fig. 2(e) is accompanied with a fainter twofold pattern, appearing in the left side of the single LID structure. We consider that the single LID structure extends in the thin foil, turning out to be the doubled LID structure in part. Since the thickness of the specimen is estimated to be about 10 nm, the defect includes at most 10^2 agglomerated self-interstitials. After irradiation for 1260 s [Fig. 2(c)], the defect was slightly extended and exhibited its habit plane, i.e., {113}-type plane. The corresponding processed image in Fig. 2(f) shows that a sequence of the three *I* structures (marked by the longer arrows) are nucleated in the regular lattice. The faint image pattern denoted by the shorter arrow is probably due to the incomplete lattice reconstruction leading to the eight-membered ring, or the *O* structural unit which is definitely required for the extension of the defects on the {113}-type plane.[11,12] The HRTEM observation at 450 °C indicates that (1) the agglomeration of self-interstitials is initiated by forming the isolated LID structure; (2) a more symmetrical agglomerate structure, for instance, a defect on {001}, is not observed at this stage, and (3) the agglomeration proceeds by the successive nucleation of the *I* units side by side with the two *E* units always attached at both ends of a sequence.

IV. DISCUSSION

We have suggested from the image analysis that self-interstitials are arranged along ⟨110⟩ at the early stage of agglomeration. The configuration possesses lower symmetry than usually expected; C_i for the single and the tripled LID, and C_{2h} for the doubled LID, the rotational axis being along not ⟨001⟩ but ⟨110⟩. Nevertheless, the estimated energy increase per self-interstitial, 1.60 or 1.16 eV,[12] respectively, for the single or doubled LID structure is satisfactorily smaller than that estimated for an isolated self-interstitial.[15] The configuration differs from

the linear defect models of self-interstitials proposed earlier.[16,17] The LID structures consist of the five- and hexagonal (a one-element wurtzite) six- and seven-membered rings. The more extended defect structures with the hexagonal six-membered rings, which have been discussed[18,19] based on the idea[18] that the phase transformation leading to a hexagonal phase occurs involving self-interstitial, are accounted for by the extension of the LID structure in several possible ways, as has been speculated[14] and confirmed in part by this experiment. The early stage of the defect nucleation has been observed by HRTEM (Refs. 20–22) at room temperature. In contrast to previous analyses,[22] we suggest that the atomic structure of the small agglomerates is fully bonded and reconstructed. It should be pointed out that the LID structures which elongate along the equivalent ⟨110⟩ directions may exhibit different image contrast in HRTEM images, even though their atomic configuration is identical.

We are aware that the twofold patterns arising from the embedded defect (Fig. 2) differ slightly from those of the penetrating defect (Fig. 3). We attribute the difference to the dynamical diffraction inside a crystal, the lattice relaxation due to the defect, and the structure at surfaces. For accurate evaluation of the effects, parameters such as the location of the embedded defect along the electron beam are needed. However, at the present time we consider that the tedious procedure to determine the parameters by an image matching technique may not offer important additional structural information.

It is well known,[2] as also demonstrated in this experiment, that the agglomerates appear after a certain incubation period during electron irradiation. The period is greatly reduced by intentional contamination of the specimen surfaces. This experimental evidence has suggested that clusters which promote the agglomeration are formed in the period, involving impurities.[2] The specimen surfaces were not controlled during electron irradiation in the present observation, and the effect of the surface contamination on the agglomeration remains unclear at the atomic level. The single LID structure depicted in Fig. 4 leaves the dangling bonds at its ends, since the HRTEM analysis has ambiguity about the interface, normal to the electron beam, between the defect and the perfect crystal and about the existence of impurity atoms. The ends may commensurate to core structures with impurity atoms at the early stage of agglomeration. A possible model for the nuclei is the thermal donors, which are currently considered[4] to be the cluster of a self-interstitial and two oxygen atoms.

V. CONCLUSION

We have observed an early stage of the agglomeration of self-interstitials in Si by HRTEM at 450 °C. Based on the analysis of the images, we have suggested that self-interstitials are first arranged along ⟨110⟩, forming an isolated LID structure. Despite much ongoing speculative argument about the core structure of the agglomerates, the LID configuration, the smallest agglomerate structure of self-interstitials ever revealed by experiment, stimulates both experimental and theoretical studies about the variety of interaction among foreign atoms and self-interstitials in Si at the atomic level.

ACKNOWLEDGMENTS

Electron (2 MeV) irradiation was carried out at the High Voltage Electron Microscope Center of Osaka University. A part of the present work was supported by the Grant-in-Aid for Scientific Research from the Ministry of Education, Science and Culture.

APPENDIX

Electron intensity at the point $\mathbf{r}$ on the image plane, which depends on both $\mathbf{R}_i$, the location of the ith atom, and the electron optical parameters, can be represented according to the weak-phase object approximation[23] to be

$$I(\mathbf{r};\mathbf{R}_1,\mathbf{R}_2,\ldots,\mathbf{R}_n)\approx 1-2\sigma\sum_i^n \delta(\mathbf{r}-\mathbf{r}_i)^*\phi_{\text{atom}}(\mathbf{r})$$
$$=I_{\text{perfect}}(\mathbf{r})+I_{\text{defect}}(\mathbf{r}) ,$$

in which $\mathbf{r}_i$ is the component of $\mathbf{R}_i$ parallel to the image plane, σ the interaction coefficient, $*$ the convolution integral, and ϕ_{atom} the electrostatic potential resulting from an atom. The summing over the atoms constituting a perfect crystal and the defect structures separately leads the last expression. The approximation is operative for a thin specimen, even though the dynamical diffraction inside a crystal and the aberration and defocus of electron optics smear the ideal projection of the two different structures overlapped along the electron beam. The intensity of the regular lattice, I_{perfect}, could easily be subtracted from the observed images [(such as Figs. 2(a), 2(b), and 2(c)] by the Fourier filtering: In the Fourier transform of the image intensity, the sharp peaks due to the regular lattice were masked except the central peak of the zero spatial frequency, and then the rest of the spectra was synthesized by the reverse Fourier transform.

[1] G. D. Watkins, in *Proceedings of the Internatinal Conference on Lattice Defects in Semiconductors, Freiburg, 1974,* edited by F. A. Huntley, IOP Conf. Proc. No. 23 (Institute of Physics and Physical Society, London, 1975), p. 1.

[2] M. Hasebe, R. Oshima, and F. E. Fujita, Jpn. J. Appl. Phys. **25**, 159 (1986).

[3] M. Reiche, J. Reichel, and W. Nitzshe, Phys. Status Solidi A **107**, 851 (1988).

[4] P. Deák, L. C. Snyder, and J. W. Corbett, Phys. Rev. B **45**, 11 612 (1992).

[5] J. L. Lindström and T. Hallberg, Phys. Rev. Lett. **25**, 2729 (1994).

[6]M. D. Matthews and S. J. Ashby, Philos. Mag. A **27**, 1313 (1973).
[7]I. G. Salisbury and M. H. Loretto, Philos. Mag. A **39**, 317 (1979).
[8]A. Ourmazd, W. Schröter, and A. Bourret, J. Appl. Phys. **56**, 1670 (1984).
[9]T. Kamino and H. Saka, Microsc. Microanal. Microstruct. **4**, 127 (1993).
[10]C. A. Ferreira Lima and A. Howie, Philos. Mag. **34**, 1057 (1976).
[11]S. Takeda, Jpn. J. Appl. Phys. **30**, L639 (1991).
[12]M. Kohyama and S. Takeda, Phys. Rev. B **46**, 12 305 (1992).
[13]S. Takeda, M. Kohyama, and K. Ibe, Philos. Mag. A **70**, 287 (1994).
[14]S. Takeda, S. Muto, and M. Hirata, in Proceedings of the 16th International Conference on Defects in Semiconductors 16, Lehigh, 1991, edited by G. Davies, G. G. Deleo, and M. Stavola [Matter. Sci. Forum **83-87**, 309 (1992)].
[15]For instance, P. J. Kelly and R. Car, Phys. Rev. B **45**, 6543 (1992).
[16]J. W. Corbett and J. C. Bourgoin, in *Point Defects in Solids,* edited by J. H. Crawford, Jr. and L. M. Slifkin, Semiconductors and Molecular Crystals Vol. 2 (Plenum, New York, 1975), p. 1.
[17]T. Y. Tan, Philos. Mag. A **44**, 101 (1981).
[18]A. Bourret, in *Microscopy of Semiconducting Materials,* edited by A. G. Cullis and D. B. Holt (Institute of Physics, London, 1987), p. 39.
[19]A. Parisini and A. Bourret, Philos. Mag. A **67**, 605 (1994).
[20]K. Hiraga and M. Hirabayashi, in *Proceedings of the 7th International Conference on High Voltage Electron Microscopy,* edited by R. M. Fisher, R. Gronsky, and K. H. Westmacott (Lawrence Berkeley Laboratory, University of California, Berkeley, 1983), p. 175.
[21]M. Kuwabara, H. Endoh, Y. Tsubokawa, H. Hashimoto, Y. Yokota, and R. Shimizu, in *Proceedings of the International Symposium on "Behavior of Lattice Imperfection in Materials–In situ Experiments with HVEM,"* edited by H. Fujita (Research Center for Ultra-High Voltage Electron Microscopy, Osaka University, 1985), p. 341.
[22]P. Wener, M. Reiche, and J. Heydenreich, Phys. Status Solidi A **137**, 533 (1993).
[23]J. M. Cowley, *Diffraction Physics,* 2nd ed. (North-Holland, Amsterdam, 1981).

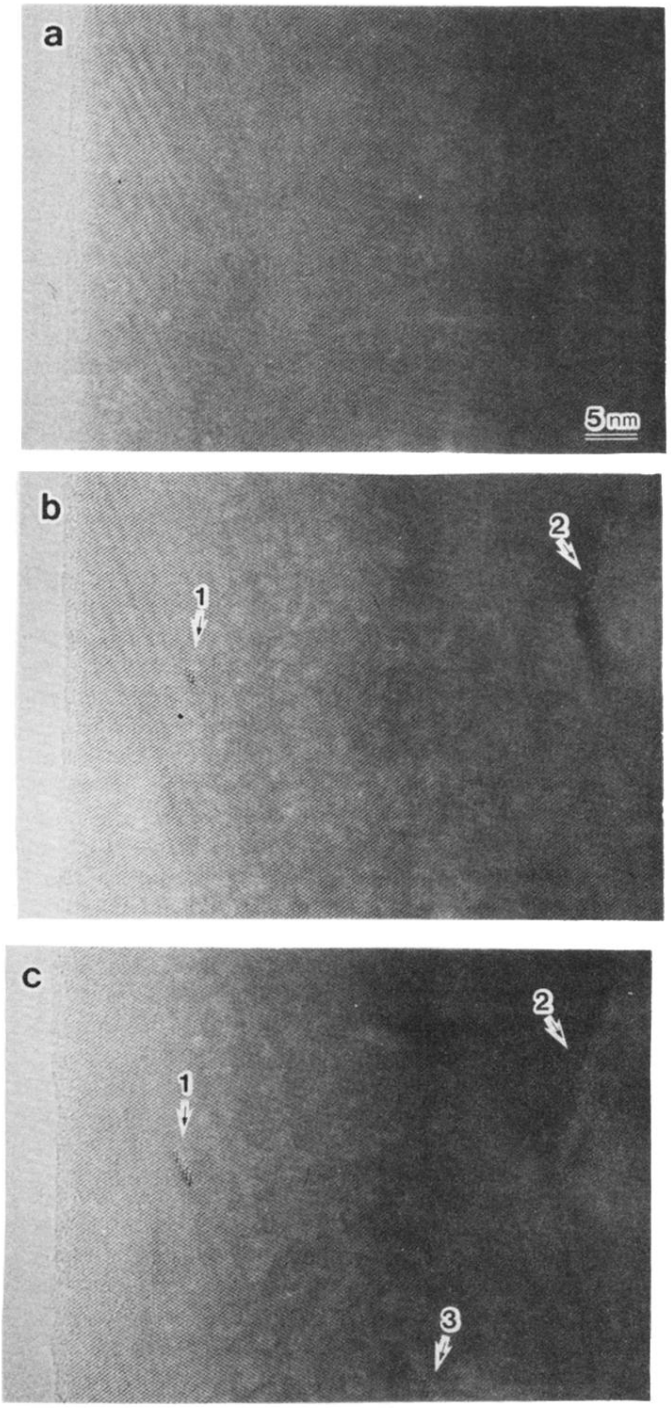

FIG. 1. Agglomeration process revealed by *in situ* HRTEM (300 kV) observation at 450 °C.

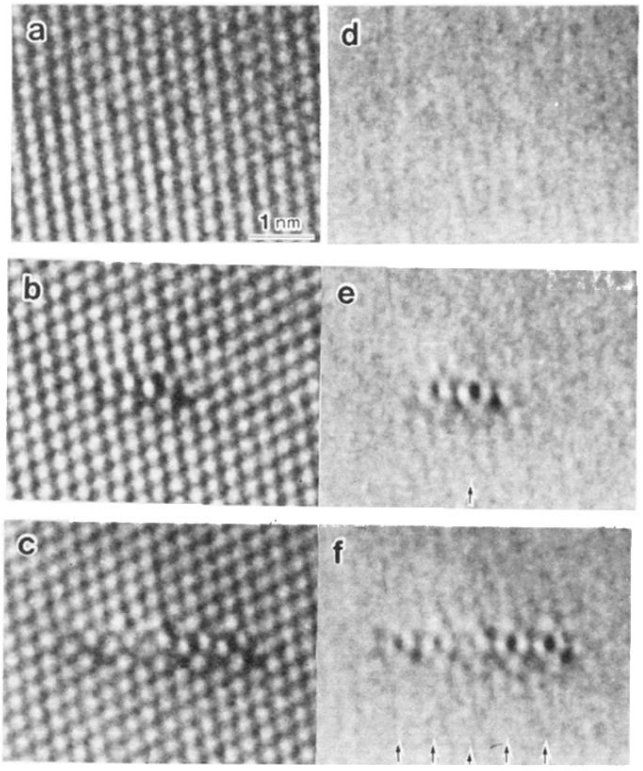

FIG. 2. Enlarged and processed images of the agglomerate 1 seen in Fig. 1.

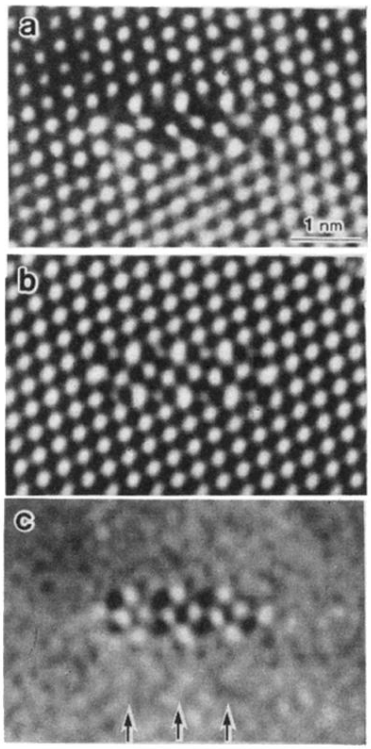

FIG. 3. Defect due to electron (2 MeV) irradiation at 450 °C observed with 160 keV electrons at room temperature.

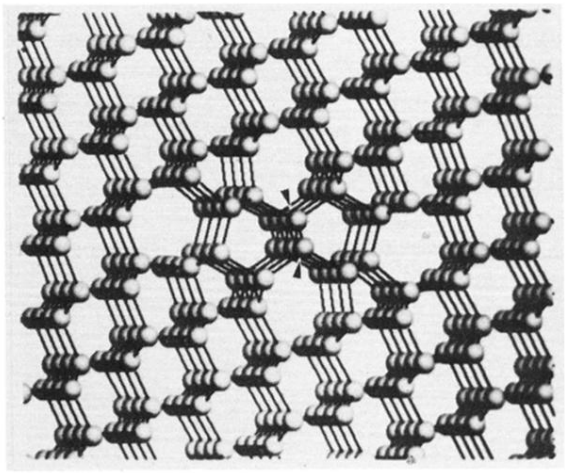

FIG. 4. The line interstitial defect configuration incorporated with self-interstitials in Si. The chain of additional Si atoms is marked by the arrow heads.